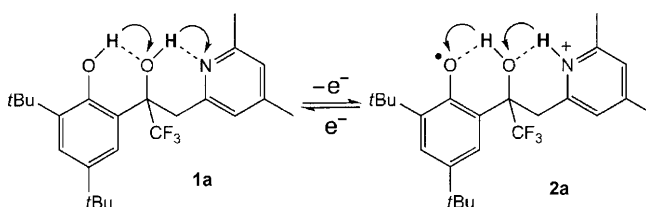


Inserting a Hydrogen-Bond Relay between Proton Exchanging Sites in Proton-Coupled Electron Transfers**

Cyrille Costentin, Marc Robert, Jean-Michel Savéant,* and Cédric Tard

Long-distance electron^[1] and proton transfer (or transport)^[2] are key processes in a considerable number of natural systems. When electron- and proton-transfer processes are coupled and involve different sites (proton-coupled electron transfer (PCET) reactions),^[3] the occurrence of concerted proton–electron transfer (CPET) reactions usually require the presence of a hydrogen bond between the proton borne by the group being oxidized and the proton acceptor (and vice versa for a reduction process), as it appears to be the case in emblematic systems such as photosystem II^[4] and ribonucleotide reductase.^[5] The distances over which the proton may travel as the result of a CPET reaction are limited to values that usually induce the formation of a hydrogen bond in the starting molecule.

Herein we explore the idea according to which this distance might be substantially increased by inserting a hydrogen-bond relay between the group being oxidized and the distant proton acceptor as represented in Scheme 1.^[6a,b] The relay is a group bearing a hydrogen atom, able to accept a hydrogen bond from the moiety being oxidized and, at the same time, able to form a hydrogen bond with the proton accepting group without going through a protonated state in the course of the reaction.



Scheme 1.

Although other moieties could play a similar function, we have selected an OH group for this purpose—having in mind

the role sometimes invoked of water molecules in PCET reactions.^[7] The molecule in Scheme 1 does not retain the properties of chains of water molecules engaged in a Grotthuss-type transport of a proton,^[8] however the OH group possesses the basic property of water molecules in that it is both a hydrogen-bond acceptor and donor.

To test the occurrence of the reaction depicted in Scheme 1 we chose to use the electrochemical approach for the PCET reactions^[3b,9] rather than the homogeneous approach. The main reason for this choice of nondestructive electrochemical techniques, such as cyclic voltammetry measurements,^[10] is the quick investigation of a continuous range of driving forces that leads to the determination of a standard rate constant (rate constant at zero driving force). The main features of the typical cyclic voltammogram shown in Figure 1a are a one-electron stoichiometry (determined from the peak height) and chemical reversibility, thus indicating that the cation radical **2a** resulting from oxidation is stable on the cyclic voltammetric time scale. Species **2a** is actually stable for longer periods of time as revealed by preparative-scale electrolysis^[6c] at 1.34 V vs. NHE. These results confirmed the one-electron stoichiometry and the formation of the expected radical cation **2a**, which is characterized by a typical UV/Vis spectrum for a phenoxyl radical species^[11] (λ : 389, 407, 645 nm; ϵ : 1507, 1549, 164 L cm⁻¹ mol⁻¹). The infrared spectrum of **2a** shows the depletion of a band at 1631 cm⁻¹ corresponding to a C=C vibration of the pyridine moiety (the second pyridine C=C band is hidden by the supporting electrolyte). The same evolution was observed upon protonation of 2,4,6-trimethylpyridine (band at 1633 cm⁻¹), thus confirming that the pyridine moiety is protonated upon generation of the phenoxyl radical species.

The reversibility and one-electron stoichiometry of the cyclic voltammetric response shown in Figure 1a contrasts with the irreversibility and two-electron stoichiometry observed when neither the pyridine acceptor, nor the OH relay are present as with 2,4,6-tri-*tert*-butyl phenol (**1c**; Figure 1c). For **1c**,^[12] the cation radical that was initially generated rapidly and irreversibly deprotonates, and the resulting phenoxyl radical is oxidized more easily than the starting phenol according to an ECE mechanism,^[10] thus resulting in a two-electron stoichiometry. The same behavior is also observed in the presence of the OH relay and in the absence of the pyridine moiety (Figure 1d; the synthesis of **1d** is described in the Supporting Information). It also follows that the reversible oxidation of **1a** does not proceed through the intermediacy of the cation radical bearing a positive charge on the central OH group.

[*] Prof. Dr. C. Costentin, Prof. Dr. M. Robert, Prof. Dr. J.-M. Savéant, Dr. C. Tard
Laboratoire d'Electrochimie Moléculaire, Unité Mixte de Recherche Université – CNRS No 7591, Université Paris Diderot, Bâtiment Lavoisier
15 rue Jean de Baïf, 75205 Paris Cedex 13 (France)
E-mail: saveant@univ-paris-diderot.fr

[**] Financial support from the Agence Nationale de la Recherche (Programme blanc PROTOCOLE) is gratefully acknowledged.

Supporting information for this article is available on the WWW under <http://dx.doi.org/10.1002/ange.200907192>.

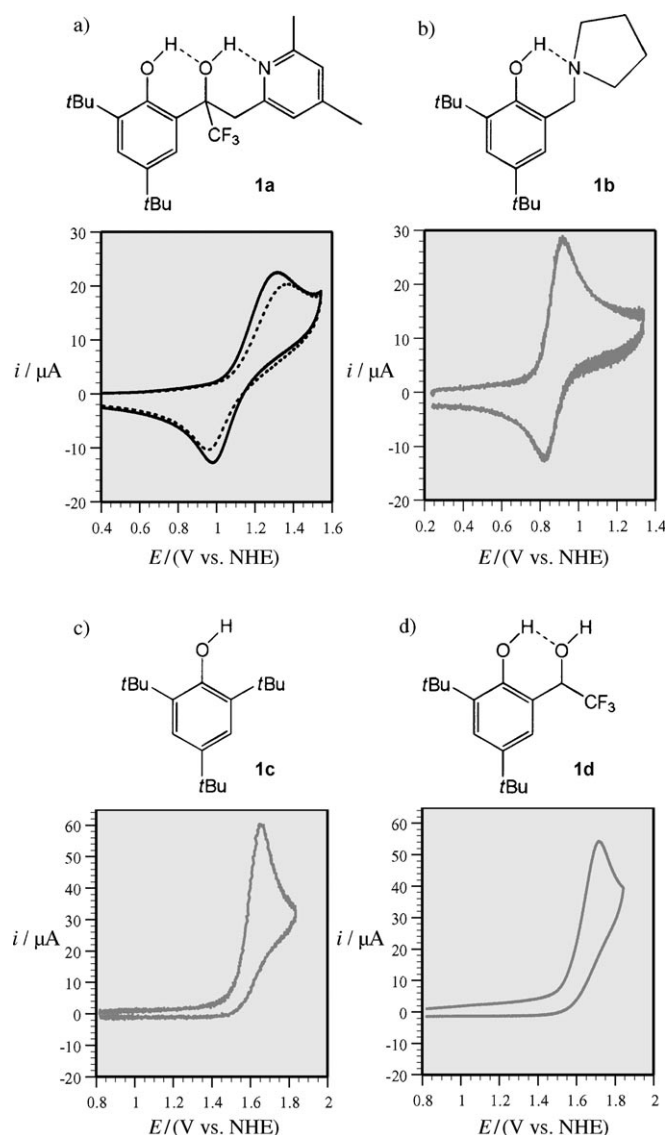


Figure 1. Cyclic voltammetry measurements in acetonitrile + 0.1 M $n\text{Bu}_4\text{NBF}_4$ for 1 mM of compound at a glassy carbon electrode and at a scan rate of 0.2 V s^{-1} . In the scan of **1a**, the solid and dashed traces were recorded in the presence of 1% CH_3OH or CD_3OD , respectively.

The cyclic voltammetric response of **1a** (Figure 1a) resembles more that of the aminophenol **1b** (Figure 1b) in terms of both electron stoichiometry and chemical reversibility, although the anodic-to-cathodic potential separation is larger in the first case than in the second. As shown earlier,^[13,14] with **1b**, the proton generated upon one-electron oxidation of the phenol moiety is transferred to the amine group concertedly with electron transfer thanks to a six-membered ring configuration, which is favorable to the formation of a hydrogen bond between the phenol and amine group in the starting molecule. In the case of **1a**, proof that the alcoholic OH group effectively serves as a hydrogen-bond relay between the phenol and pyridine groups requires that the molecule is not folded so as to put these two groups at a sufficiently short distance from one another to bring about

the direct formation of a hydrogen bond between them. The X-ray structure of **1a**^[6b] (Figure 2) shows that this is indeed the case—the distance between the phenolic oxygen atom and

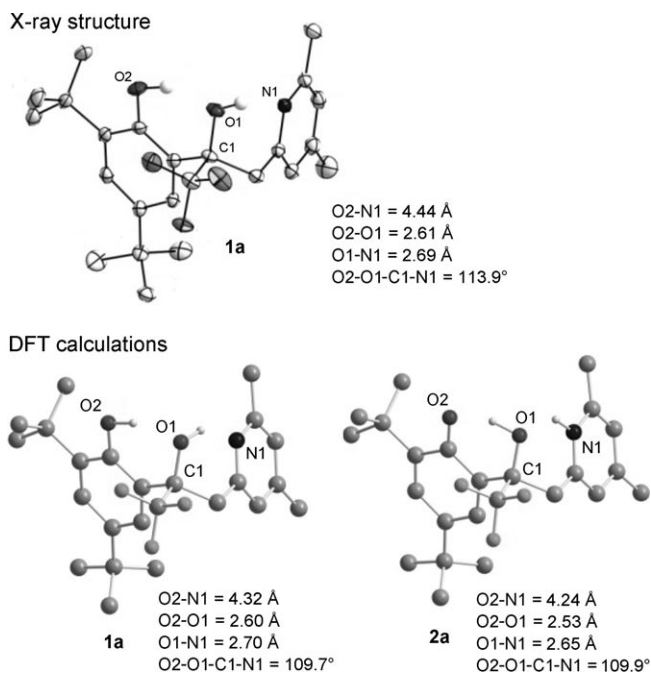
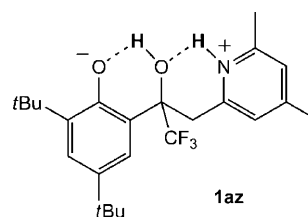


Figure 2. X-ray structure^[6] of **1a** and DFT calculations^[10] for **1a** and **2a**.

the nitrogen atom of pyridine is indeed 4.44 Å and the O2-O1-C1-N1 dihedral angle is 113.9° . The DFT calculations^[6c] led to a very similar result in the case of **1a** (Figure 2) and also showed that substantial folding does not take place in cation radical **2a**.

Another interesting observation is that of the existence of an H/D kinetic isotope effect (KIE) for **1a**—similar to what was observed with **1b** (see Table 1)—thus pointing to the occurrence of a concerted pathway indicating that the equilibrium shown in Scheme 1 is not merely the expression of a global process but should be viewed as an elementary CPET step. This conclusion also falls in line with the implausibility of a mechanism that would proceed through oxidation of the zwitterionic form (**1az**) of **1a**, owing to the small equilibrium ratio $[\mathbf{1az}]/[\mathbf{1a}] \approx 10^{-9}$.^[15] Also, the fact that the reaction does not proceed via an intermediate in which the central OH group is protonated is in agreement with the $\text{p}K_a$ values of phenol ($\text{p}K_a = 27$)^[15a] and protonated alcohol ($\text{p}K_a < 2$)^[15d] in acetonitrile.



In the framework of the CPET mechanism, we derive the standard rate constant of the reaction (k_s) from the peak separation in Figure 1a, after linearization of the Marcus–Hush–Levich activation-driving force law, thus leading to the Butler–Volmer rate law^[6c,13b] with a transfer coefficient equal to 0.5 [Eq. (1)]; where i : current, S : electrode surface area, $[]$: concentrations at the electrode surface, E : electrode potential, E^0 : CPET standard potential. The standard rate constant of the reaction (k_s), that is, the rate constant at zero driving force, is a measure of the intrinsic characteristics of the reaction.

$$\frac{i}{FS} = k_s \exp\left[\frac{F}{2RT}(E - E^0)\right] \left\{ [1] - \exp\left[\frac{-F}{RT}(E - E^0)\right] [2] \right\} \quad (1)$$

It is immediately clear that with **1a**, a scan rate of only 0.2 V s⁻¹ is sufficient for the peak separation to be controlled by the CPET kinetics (Figure 1a). Whereas at this scan rate, the oxidation of **1b** is still controlled by diffusion (Figure 1b). For **1b**, one has to operate at a scan rate of 5 V s⁻¹ to reach the CPET kinetic control to achieve good peak separation.^[13] Table 1 summarizes the values of k_s obtained by using, as the

Table 1: Characteristics of the CPET oxidation of **1a** and **1b**.

Compound	E^0 [V/NHE ⁻¹]	$k_{s,H}$ [cm s ⁻¹]	KIE	λ [eV]	λ_0 [eV]	λ_i [eV]
1a	1.10	5×10^{-4}	2.4	1.36	0.78	0.58
1b ^[13]	0.85	8×10^{-3}	1.7	1.06	0.78	0.28

diffusion coefficient the value derived from the peak heights (10⁻⁵ cm² s⁻¹), together with the values of the standard potential. Comparison between the values of k_s in the presence of 1% of CH₃OH or CD₃OD allowed the determination of the H/D kinetic isotope effects reported in Table 1 (upon introduction of 1% of CD₃OD, the NMR proton signals for phenol and alcohol disappeared therefore indicating complete deuteration).

With such a small KIE and assuming that electron transfer is adiabatic,^[13b] the preexponential factor (Z) in the expression of the standard rate constant (as illustrated experimentally by the temperature dependent kinetics of the oxidation of **1b**^[13b]) [Eq. (2)]^[10,13c] can be approximated by the collision

$$k_s = Z \sqrt{\frac{RT}{4\pi\lambda}} \int_{-\infty}^{\infty} \frac{\exp\left[-\frac{RT}{4\lambda} \left(\frac{\lambda}{RT} - \zeta\right)^2\right]}{1 + \exp(\zeta)} d\zeta \quad (2)$$

frequency, $Z = \sqrt{RT/2\pi M}$ (M : molar mass, $M = 423$ g mol⁻¹), thus leading to a numerical estimation of the experimental reorganization energy, $\lambda = 1.36$ eV for **1a**, to be compared with $\lambda = 1.06$ eV for **1b**. The solvent reorganization energy (λ_0) has been estimated to be 0.78 eV for **1b**, and is likely to be the same for **1a**. It follows that the internal reorganization energy varies from 0.28 to 0.58 eV from **1b** to **1a**. With a more rigid structure, in which the movements of the heavy atoms would be minimized, the standard rate

constant for **1a** should therefore be marginally slower than for **1b**.

We may thus conclude that the introduction of a hydrogen bonding group between the electron and proton exchanging sites may offer an efficient route for proton movement over distances as large as 4.3 Å, by means of the translocation of two protons in a concerted manner with electron transfer. This Grotthuss-type proton transfer is as efficient as the travel a proton accomplishes over distances of the order of 2.5 Å in systems where hydrogen bonding between the phenol moiety and the proton acceptor benefits from the formation of a six-membered ring. The key feature of this efficient proton movement is a “hydrogen-bond swing” as the one shown in Scheme 1, which avoids going through a high-energy intermediate in which the relay would be protonated. The ability of the trifluoro-substituted alcohol group to serve as an efficient relay is presumably the result of a good balance between its hydrogen-bond-accepting and -donating capabilities.

Work is in progress to further investigate the mechanism of the hydrogen-bond relay and to uncover the parameters that constitute a good relay.

Received: December 21, 2009

Published online: April 20, 2010

Keywords: electrochemistry · electron transfer · hydrogen bonds · phenols · proton transfer

- [1] a) H. B. Gray, J. R. Winkler, *Q. Rev. Biophys.* **2003**, *36*, 341–372; b) C. C. Page, C. C. Moser, P. L. Dutton, *Curr. Opin. Chem. Biol.* **2003**, *7*, 551–556.
- [2] C. A. Wraight, *Biochim. Biophys. Acta Bioenerg.* **2006**, *1757*, 886–912.
- [3] a) S. Y. Reece, D. G. Nocera, *Annu. Rev. Biochem.* **2009**, *78*, 673–699; b) C. Costentin, *Chem. Rev.* **2008**, *108*, 2145–2179.
- [4] A. W. Rutherford, A. Boussac, *Science* **2004**, *303*, 1782–1784.
- [5] J. Stubbe, D. G. Nocera, C. S. Yee, M. C. Y. Chang, *Chem. Rev.* **2003**, *103*, 2167–2202.
- [6] a) The synthesis of **1a** is described in the Supporting Information; b) CCDC 746981 (**1a**) contains the supplementary crystallographic data for this paper. These data can be obtained free of charge from The Cambridge Crystallographic Data Centre via www.ccdc.cam.ac.uk/data_request/cif; c) see Supporting Information.
- [7] M. Wang, J. Gao, P. Müller, B. Giese, *Angew. Chem.* **2009**, *121*, 4296–4298; *Angew. Chem. Int. Ed.* **2009**, *48*, 4232–4234.
- [8] a) J. T. Hynes, *Nature* **2007**, *446*, 270–273; b) D. Marx, *ChemPhysChem* **2006**, *7*, 1848–1870.
- [9] a) S. Wang, P. S. Singh, D. H. Evans, *J. Phys. Chem. C* **2009**, *113*, 16686–16693; b) C. Costentin, C. Louault, M. Robert, J.-M. Savéant, *Proc. Natl. Acad. Sci. USA* **2009**, *106*, 18143–18148.
- [10] J.-M. Savéant, *Elements of Molecular and Biomolecular Electrochemistry*, Wiley-Interscience, New York, **2006**.
- [11] a) E. R. Altwick, *Chem. Rev.* **1967**, *67*, 475–531; b) T. Maki, Y. Araki, Y. Ishida, O. Onomura, Y. Matsumura, *J. Am. Chem. Soc.* **2001**, *123*, 3371–3372.
- [12] J. A. Richards, P. E. Whitson, D. H. Evans, *J. Electroanal. Chem.* **1975**, *63*, 311–327.
- [13] a) C. Costentin, M. Robert, J.-M. Savéant, *J. Am. Chem. Soc.* **2006**, *128*, 4552–4553; b) C. Costentin, M. Robert, J. M. Savéant, *J. Am. Chem. Soc.* **2007**, *129*, 9953–9963.

- [14] a) homogenous oxidation of similar aminophenols has also been reported, see reference [14c]; b) I. J. Rhile, J. M. Mayer, *J. Am. Chem. Soc.* **2004**, *126*, 12718–12719; c) I. J. Rhile, T. F. Markle, H. Nagao, A. G. DiPasquale, O. P. Lam, M. A. Lockwood, K. Rotter, J. M. Mayer, *J. Am. Chem. Soc.* **2006**, *128*, 6075–6088.
- [15] a) $\frac{[1\mathbf{az}]}{[1\mathbf{a}]} \approx 10^{-\left(\frac{\text{p}K_{\text{PhOH}} - \text{p}K_{2,4,6\text{-trimethylpyridine}} + \text{p}K_{2,4\text{-dimethylpyridine}}}{2}\right)} \approx 10^{-9}$, approximated by extrapolation and interpolation from the $\text{p}K_{\text{a}}$ values of pyridine and phenol in acetonitrile (12.3 and 27, respectively)^[15b] and in water (5.2 and 10, respectively),^[15c] and the $\text{p}K_{\text{a}}$ values for 2,4,6-trimethylpyridine and 2,4-dimethylpyridine in water (7.43 and 6.99, respectively).^[15c] The $\text{p}K_{\text{a}}$ value used for the pyridine in **1a** was the average value for 2,4,6-trimethylpyridine and 2,4-dimethylpyridine.^[15b] b) K. Izutzu in *Acid-Base Dissociation Constants in Dipolar Aprotic Solvents*, Blackwell, Boston, **1990**, pp. 17–35; c) *Handbook of Chemistry and Physics*, 82nd ed. (Ed.: D. R. Lide), CRC, Boca Raton, **2001–2002**, pp. 8-48–8-56; d) I. M. Kolthoff, M. K. Chantooni, *J. Am. Chem. Soc.* **1968**, *90*, 3320–3326.
- [16] Other approaches are possible, see for example: S. Hammes-Schiffer, A. V. Soudackov, *J. Phys. Chem. B* **2008**, *112*, 14108–14123.